

Advancing Electronic Application of Coordination Solids: Enhancing Electron Transport and Device Integration via Surface-Mounted MOFs (SURMOFs)

Zhengtao Xu,^{*} Christof Wöll,^{*} and Stefan Bräse^{*}

The layer-by-layer (LbL) assembly of coordination solids, enabled by the surface-mounted metal–organic framework (SURMOF) platform, yields thin films with well-defined orientation, tunable thickness, low density of defects, and editable crystalline heteroepitaxy. Such high-quality thin films are suited for integrating metal–organic framework (MOF) materials into devices used in electronics and optoelectronics technologies. However, the potential of the SURMOF platform has not been fully realized due to its instability, poor electronic interaction/transport, and limited intercalation/heteroepitaxy functions. Leveraging the longstanding efforts in processing and functionalizing coordination networks, four directions are highlighted for fully unleashing the technological potential of the SURMOF platform: 1) cascade cyclization to form polycyclic aromatic, nanographene-like scaffolds with strong electron polarizability and electroactivity; 2) crosslinking by fused-aromatic and metal–thiolate bridges for improved charge transport and structural stability; 3) covalent-ionic heteroepitaxy of conductive metal–thiolate layers alternating with metal–aqua-hydroxide layers to emulate the transport layer and the charge storage layer in high-temperature superconductors of cuprates and iron pnictides; and 4) machine learning (ML)-based methods to optimize synthesis conditions.

The template-guided assembly of building blocks into materials is essential for life and civilization, as demonstrated by the 550-million-year history of biomineralization in which organisms form shells and skeletons from calcium carbonate and phosphate.^[1,2] The notably gentle conditions under which natural biomineralization occurs are motivating the search for less severe methods of processing ceramics^[3,4] as alternatives to the

intense, high-temperature firing and sintering techniques currently in use. Plastics, by comparison, are easier to process, leading to their widespread use in industry and everyday life.

With electronics technology, the processing of semiconductors, superconductors, and other materials into thin films is essential for device fabrication as well as for fundamental studies. These workhorse materials (e.g., Si and GaAs) are usually robust, close-packed inorganic solids that must be deposited from the gas phase to form thin films onto substrates. To control the film thickness or composition of these refractory inorganic solids (as in atomic layer deposition and epitaxy thin film growth), complex high-vacuum apparatuses are needed.^[5] The weaker-bonded inorganics, such as the lead halide perovskites (widely studied for photovoltaics and luminescence devices), are easier to process (e.g., by solution deposition from acetone)^[6–8] but are inherently less stable, limiting their durability and reliability in practical applications.

Moreover, like many inorganic solids, they lack modifiable functional groups for improving their stability (e.g., by crosslinking^[9]); and they are usually close-packed, non-porous structures and thus do not readily accommodate guest molecules for modifying their properties or increasing stability.

Metal–organic frameworks (MOFs; aka coordination polymers)^[10–19] can overcome the limitations in processability,

Z. Xu^[+]

Institute of Materials Research and Engineering (IMRE)
Agency for Science Technology and Research (A*STAR)
2 Fusionopolis Way, Singapore 138634, Singapore
E-mail: zt.xu@siat.ac.cn

 The ORCID identification number(s) for the author(s) of this article can be found under <https://doi.org/10.1002/adfm.202425091>

^[+]Present address: Shenzhen Institute of Advanced Technology, Chinese Academy of Sciences, Shenzhen, Guangdong 518055, China

© 2025 The Author(s). Advanced Functional Materials published by Wiley-VCH GmbH. This is an open access article under the terms of the [Creative Commons Attribution](#) License, which permits use, distribution and reproduction in any medium, provided the original work is properly cited.

DOI: 10.1002/adfm.202425091

C. Wöll

Institute of Functional Interface
Karlsruhe Institute of Technology (KIT)
Kaiserstrasse 12, 76131 Karlsruhe, Germany
E-mail: Christof.Woell@KIT.edu

S. Bräse

Institute of Organic Chemistry
Kaiserstrasse 12, 76131 Karlsruhe, Germany
E-mail: braese@kit.edu

S. Bräse

Institute of Biological and Chemical Systems—Functional Molecular Systems
Karlsruhe Institute of Technology
Kaiserstrasse 12, 76131 Karlsruhe, Germany

functionality, and porosity of inorganic solids. MOFs have tunable bonding strength of the coordination links, versatile organic functions, and well-defined open structures, all of which offer broad possibilities for processing and modifications. In general, the coordination bonds or linkages in MOFs are a two-edged sword. On the one hand, the reversible coordination bonds facilitate solution-based processing, as well as the crystallization of well-defined, ordered infinite structures in the solid state. This provides crystalline samples for structural elucidation, e.g., by X-ray diffraction. On the other hand, such reversible and labile links limit not only the stability of the framework structure but also the electronic interaction across the metal center and the organic linker molecule. In addition, the density of defects is often difficult to control.

This limited stability, together with high costs, disadvantages MOF solids in comparison with activated carbon, zeolites, and other established open-structure materials (swollen crosslinked polymers/ion-exchange resin, Prussian blue analogs) in sorption/separation and other heavy-duty industrial applications. Instead of competing against these mass-produced industrial materials, here we capitalize on the ease of processing and rich functionalities of coordination solids, in order to generate fresh insights for chemistry and materials research and to tease out the deeper impacts of this busy field.

The ease of processing (enabled by the labile coordination links) implies structural fragility, but the organic linker molecules can be flexibly equipped with cross-linkable groups, not only to reinforce/stabilize the MOF scaffold, but also to improve materials properties such as electronic interaction throughout the solid state. In this light, the development of processing methodologies and the design of functional molecular building blocks stand out as two key drivers in the field. Of strategic importance is the synergism of these two lines of endeavors, as a functional design can not only generate fundamental insights (such as site isolation for heterogeneous catalysis^[20,21] and novel conduction medium across organic molecules^[22,23]) but also boost thin-film and related technologies when integrated with the development of processing methodologies.

The forefront of processing MOF solids is best epitomized by the liquid-phase epitaxy (LPE) layer-by-layer (LbL) deposition of surface-mounted MOFs (SURMOFs).^[24–26] In this technique, carefully programmed dipping-washing-dipping iterations enable controlled epitaxial growth of thin films with good monolithic uniformity and orientation (Figure 1).^[27] The protocol was first developed for depositing the more labile Cu(II)-carboxylate frameworks,^[24] but advances in the field have been rapid; even the very robust frameworks based on the strong Zr(IV)-carboxylate links (e.g., UiO-66-NH₂) can now be processed into uniform, continuous SURMOF films by the LPE method (Figure 1).^[27] The high-quality UiO-66-NH₂ film thus obtained remains intact even after exposure to boiling water for 1 h. The resulting stable, pinhole-free thin film of UiO-66-NH₂ is important for membrane technology, as MOF membranes processed from powder often suffer leakage from pinholes or weaker stability compared with the bulk form. For example, the crystallites of the zeolitic imidazolate framework (ZIF) Zn(2-methylimidazolate)₂, ZIF-8, slowly dissolve in water, and its thin films dissolve even faster.^[27,28]

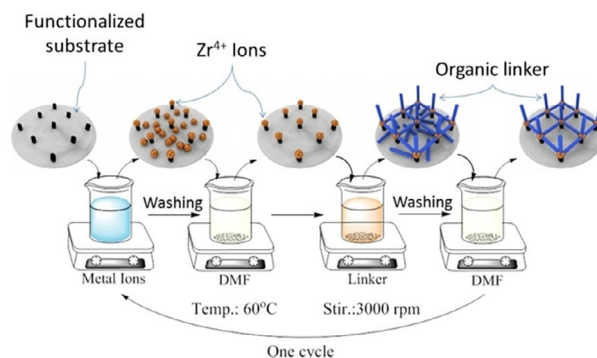


Figure 1. Schematic diagram for the synthesis of UiO-66-NH₂ SURMOF through LPE.

Here, we use the example of Figure 1 to illustrate the key technical aspects of the LPE deposition protocol, including substrate (e.g., by self-assembled monolayers), solvent, temperature, and the use of pre-assembled clusters as the metal node for network construction. A key parameter in the LPE synthesis of UiO thin films is the choice of a suitable solvent, DMF (N,N-dimethylformamide), together with an –OH functionalization of the substrate. Flat gold films supported on Si wafers were first functionalized by immersion in an ethanolic solution of 11-mercapto-undecanol (MUD), resulting in the formation of a self-assembled monolayer (SAM) exposing an –OH terminated stem. The functionalized gold-coated substrates were then immersed in a DMF solution of ZrCl₄ in the presence of HCl, subsequently washed with DMF, and finally immersed in a solution of the organic linker, 2-aminoterephthalic acid in DMF, as shown in Figure 1. The deposition cycle was completed by washing again with the pure DMF solvent. The overall thickness of the deposited thin films was adjusted by the number of growth cycles. The many factors affecting the experimental conditions pose challenges for reliable film growth, but, in an educational setting, they offer valuable opportunities for experimentalists to explore the conditions that optimize film qualities. More importantly, burgeoning computerized automation and robotic operations facilitate fast, high-throughput screening of film growth conditions, allowing researchers to materialize the full power of the versatile LPE protocol (see below).

With the more labile but easier to crystallize Cu(II)-carboxyl paddle-wheel-based frameworks, one can access ordered and monolithic SURMOF films under milder conditions—e.g., from ethanol at room temperature.^[24] The mild processing conditions allow for more diverse and delicate functions to be built into the SURMOF thin films and thus post-synthetic modifications that improve chemical stability and mechanical and electronic properties. SURMOF thin films (grown on solid substrates via the liquid-phase quasi-epitaxy approach) also allow easier entry of guest molecules into the pores for chemical modification, as the ordered SURMOF films often exhibit fewer surface defects/barriers that limit guest uptake.^[29]

For Stability and Conductivity: Chemical modifications that simultaneously enhance the stability and electronic properties are of interest because MOFs like the Cu(II)-carboxyl ones are relatively fragile solids with insulating properties. With enhanced electronic properties (e.g., directional charge transport),

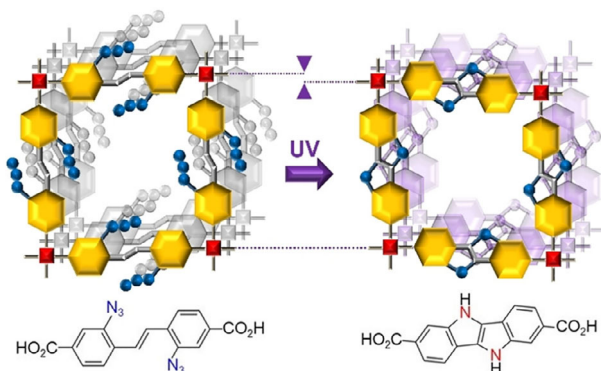


Figure 2. Schematic illustration of intramolecular photoreactions of azide in metal-organic frameworks. Red square: Cu paddle wheels; yellow hexagon: benzene ring; blue dot: nitrogen atom; gray bar: carbon bond.

SURMOF thin films stand ready for wide-ranging device application possibilities.^[26] While a number of strategies have been proposed to enhance conductivity by loading suitable molecules into the MOF pores,^[30] here we will highlight two examples of post-synthetic modifications of SURMOF thin films.

Example I: Domino Cyclization: **Figure 2** features a dicarboxyl linker molecule with reactive azide functions installed next to the alkene core. The resultant Cu(II) paddle-wheel-based SURMOF was UV irradiated under high vacuum conditions without a solvent molecule. A radical nitrene was formed, which then selectively cyclized with the adjacent C=C bond to form the fused polycyclic aromatics indoloindole. The selectivity can be ascribed to the solvent free vacuum conditions as well as the spatial restriction of the linker molecules imposed by the rigid open framework; such site isolation therefore, contrasts with the free-flowing solution regime, where the reactive azide and nitrene species randomly collide with one another to complicate the reaction landscape and product profile.

Two future directions can be envisioned from this azide-triggered functionalization of MOF solids. The first direction is toward larger fused aromatic systems for enhancing electronic properties (e.g., polarizability, mobility, and electroactivity). This can be achieved by attaching multiple neighboring alkene/alkyne units to the azide group in order to provide for domino cyclization/aromatization reactions. For example, one can use the recently reported^[31] molecule **L1** (**Figure 3**) and convert its two amino groups into azide groups using the efficient azide transfer agent trifluoromethanesulfonyl azide (i.e., triflyl azide or TfN₃). The azide-equipped linker molecule **L1a** can then be assembled (e.g., with Cu²⁺ or Zr⁴⁺ ions) into SURMOF structures, and the photochemically generated nitrene species will then trigger domino cyclization with a contiguous alkyne array. This will generate large fused aromatic π -systems linkers in the SURMOF thin-film matrix.

Earlier, similar back-folded, alkyne-rich linkers in bulk MOF powders/crystals were domino-cyclized to form nanographene links to enhance the light absorption and stability properties of the coordination solid. These cyclizations were mostly triggered by heat (e.g., 300–500 °C) without catalysts, and the resultant nanographene units are usually disordered and relatively ill-defined.^[32,33] By comparison, the azide-triggered, mild photochemical cyclization within the SURMOF confinement favors

more selective reaction pathways and a better-defined cyclization product, e.g., lower temperatures and with a rigid MOF scaffold blocking other reaction channels for the nitrene intermediate.

The more soluble azide as precursor to large aromatic linkers also serves to circumvent the solubility issue, as large aromatic molecules tend to stack closely to obviate the formation of open frameworks; i.e., it would be less feasible to directly use polycyclic fused aromatic linkers to assemble the MOF framework.

In the second direction, the rigid SURMOF host can also site-isolate and trap the nitrene as an open-shell species, as well as stabilize the derived organic radicals (e.g., from the domino cyclization process). The unpaired electrons, embedded in the large aromatic π -system of the organic linkers, as well as the high-quality thin film morphology of the SURMOF sample, offer ease and device fabrication advantages for probing and exploiting the resulting rich electromagnetic properties. Generally, there is a rising interest in stable organic radicals, both in the extended MOF framework medium and in molecular systems.^[34]

Example II: Crosslinks: The magnetic and electronic couplings throughout the solid state can be greatly enhanced with conjugated bridges across the organic linkers (as the metal-carboxyl coordination bonds do not in general provide such coupling, most MOFs are insulating and lack electroactive properties). Such conjugated crosslinking is aptly illustrated in Example II (**Figure 4**).^[35] One key motivation therein is to access polymer fabrics with interwoven fibers of monomolecular thickness. Thanks to the precise LbL deposition enabled by the LPE protocol, the dicarboxyl linker equipped with two ethynyl (C≡C–H) units and Cu(II) was deposited as a single layer into a SURMOF thin film, which is sandwiched between sacrificial MOF layers that do not contain C≡C–H units. Guest Cu(I) ions are then diffused into this multi-heteroepitaxial, crystalline thin film to effect the Glaser–Hay coupling of the C≡C–H bonds, yielding linear, interwoven polymer chains within the ordered single-layer coordination fabric. After removing the metal ions, the textile sheets can be transferred onto different supports. Imaging using scanning electron microscopy and atomic-force microscopy reveals individual polymer strands of ≈ 200 nm long.

One conceptual implication of such a synthetic exercise is symbolized by the diacetylene bridges (C≡CC≡C) formed as a conjugated pathway for promoting electronic interactions across the aromatic linker molecules. Establishing covalent links

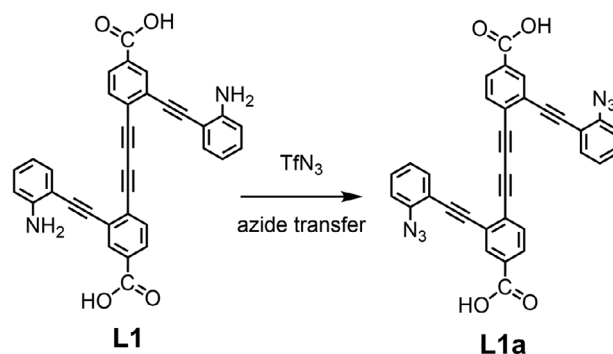


Figure 3. A proposed azide transfer reaction for accessing an alkyne-rich, azide-equipped linker molecule **L1a** for MOF construction.

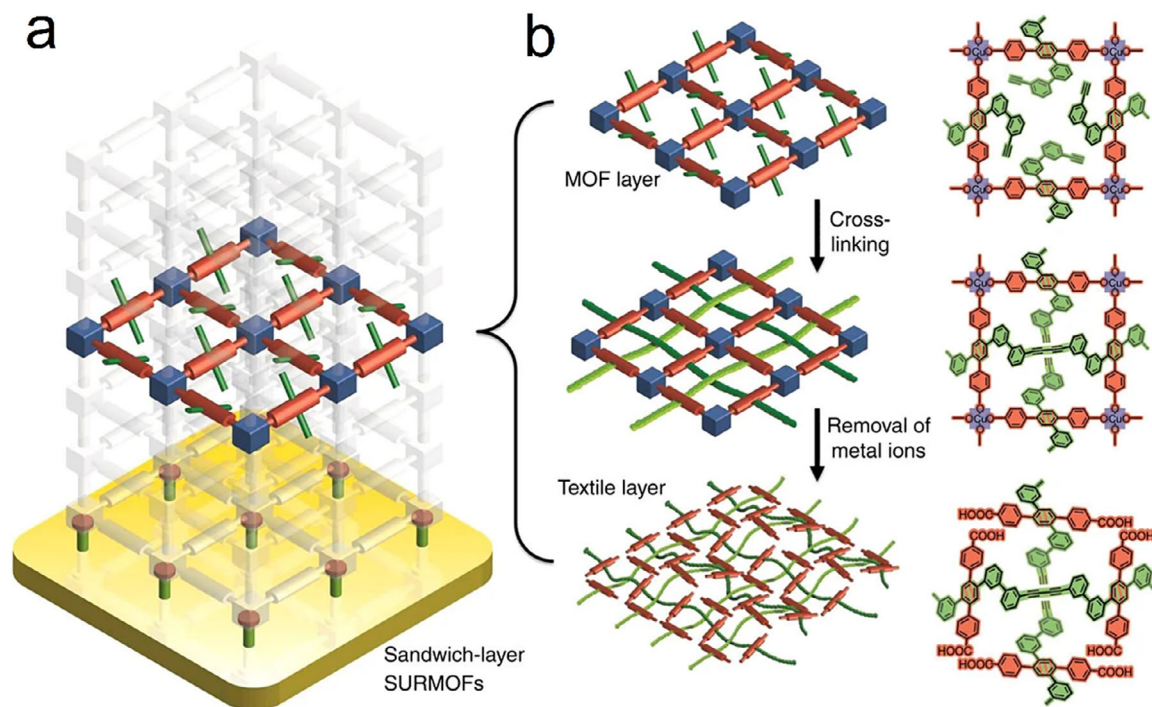


Figure 4. a) Schematic illustration of the heteroepitaxial sandwich-layer SURMOF system and b) the formation procedure of molecular weaving in the active MOF layer embedded between two sacrificial layers.

across the organic struts dates back to the early stages of work in the MOF field, as efforts to improve the framework stability and metal exchange.^[36] Subsequent crosslinking exercises have grown to include metal-thiolate and conjugated aromatic bridges across the organic struts for improving the electron transport throughout the solid state.^[9,22] The versatile processing and functionalization enabled by the SURMOF platform further open up application horizons for the crosslinking practice.

For example, the azide functions were used earlier to click-react with ethynyl units for crosslinking a SURMOF thin film, yielding a 3D, highly porous, covalently bound polymer film of homogeneous thickness.^[37] Removing the metal ions resulted in a surface-grafted gel (SURGEL) with functional pores and uniform thin-film morphology, as well as stability under biological conditions. These SURGELS can be loaded with bioactive compounds and applied as bioactive coatings, and they provide a drug-release platform in in vitro cell culture studies.

Integrating Cyclization and Crosslinking: Here, we again highlight the two key modifications of the MOF solids: 1) massive cyclization triggered by the azide-derived nitrene species to form polarizable large aromatic π -electron systems (Example I, Figure 2); and 2) direct crosslinks of the terminal alkyne groups (in the same spirit as Example II, Figure 4). Future work can combine these two fundamental transformation motifs of cyclization and crosslinking. Namely, crosslinking and further ring fusion can be forged among the domino-cyclized large- π linkers, in order to electronically integrate these large π -systems into 2D carbon ribbons or 3D carbon grids that are functionalized with the metal nodes from the MOF precursor.

The crosslink motifs are as broad as chemistry itself. For example, other crosslinks can be provided by [2.2]paracyclophane (PCP)^[38] and sulfur (or other chalcogen) side groups such as $-\text{SH}$, $-\text{S}-\text{SCH}_3$, or $-\text{S}-\text{C}\equiv\text{C}-\text{R}$ (Figure 5).^[39] The paracyclophane is known to ring-open to form (benzyl) radical intermediates $\approx 200^\circ\text{C}$.^[38,40] By attaching it to the contiguous alkyne array, as in the proposed L2, the ring-opened intermediates will trigger cyclization among the alkyne units to form extensive crosslinked polycyclic aromatic units (nanographene) in the SURMOF matrix. Moreover, the PCP substituent as shown in L2 features homochirality, which can be carried over into the cyclized/crosslinked SURMOF film as support for enantioselective catalysis applications.^[41,42]

The sulfur side groups offer a well-defined alternative to the large aromatic bridges (e.g., from cascade cyclization as mentioned above) for electronically integrating the linker π -systems.

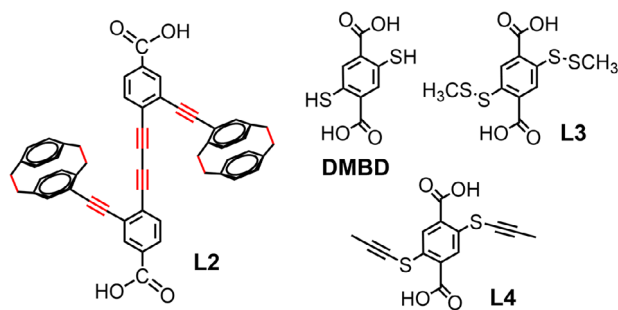


Figure 5. Four dicarboxyl linker molecules with paracyclophane (L2) and sulfur side groups (DMBD, L3, L4) for crosslinking reactions.

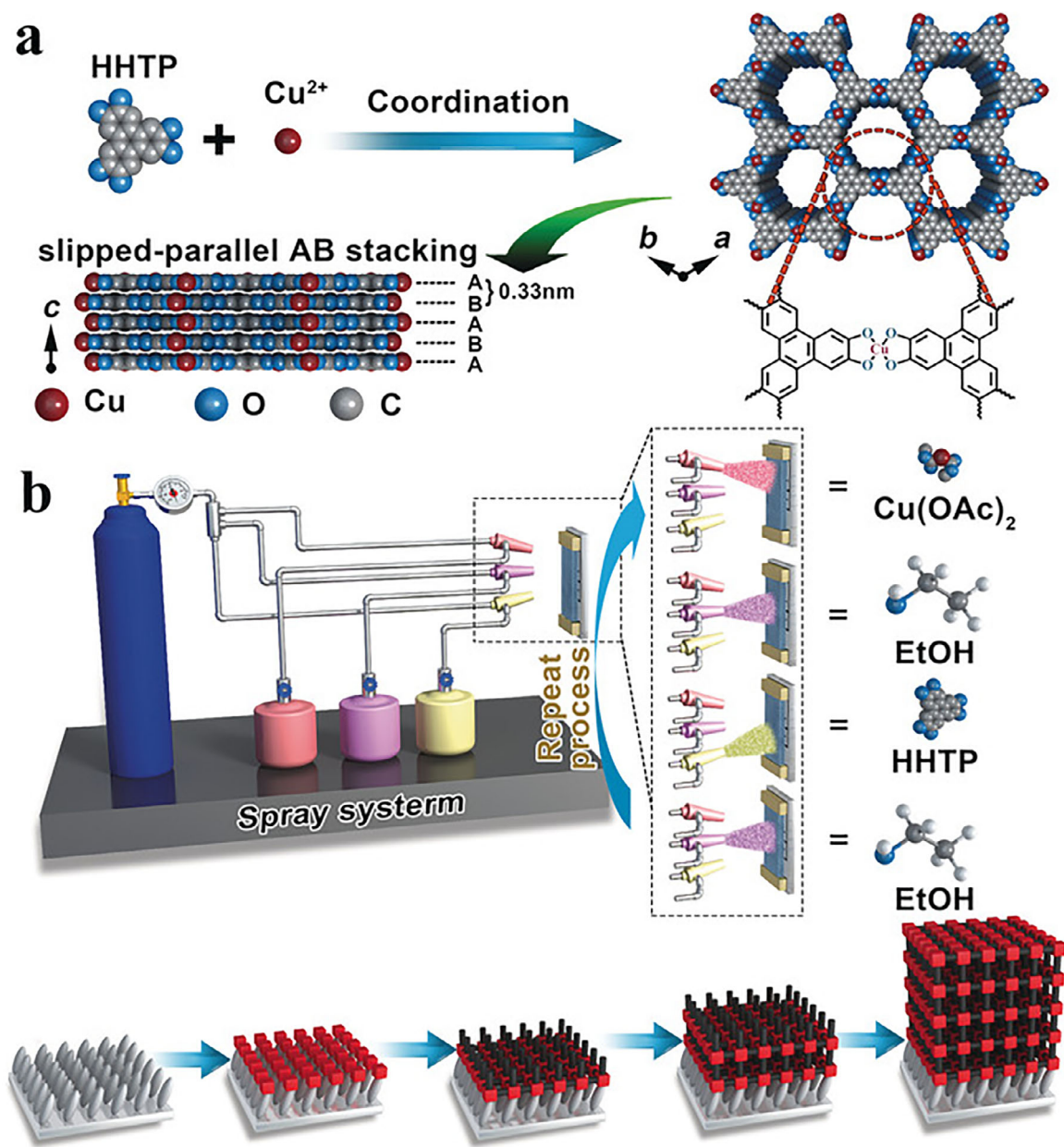


Figure 6. Illustration of a) the crystal structure of Cu₃(HHTP)₂ and b) the preparation of Cu₃(HHTP)₂ thin-film gas sensors.

For example, this can occur by way of metalation to establish electroactive S–M–S bridges, as transit metal-thiolate solids are known for their versatile electron transport and magnetic and redox activity.^[43–46] In particular, the thin-film geometry afforded by the SURMOF platform will greatly facilitate the fabrication of electronic devices and electrode-coating applications of these sulfur coordination solids. The DMBD (2,5-dimercapto-1,4-benzenedicarboxylic acid) linker molecule, as shown in Figure 5 can readily form MOF solids,^[47] such as ZrDMBD featuring accessible, free-standing mercapto groups for metal binding and functionalization. It therefore offers a good candidate for SURMOF construction. On the other hand, molecule L3 features the disulfide side groups as a protection of thiol groups to afford more stability against air oxidation. The disulfide groups are also

less prone to bonding with transition metal ions and therefore are more compatible for constructing metal-carboxylate MOF structures, e.g., based on the Cu(II)-carboxylate paddle-wheel motif. The free-standing disulfide units in the MOF pores can also react with Fe(CO)₅ and other low-valence metal species to insert functionalizing S–Fe–S units in the pores. This simple yet versatile linker molecule therefore stands as a good target and opportunity for synthetic chemists to impact the field of materials science.^[48] Finally, ligand L4, once built into a MOF or SURMOF structure, offers acetylenic sulfide functions^[49] for coordinating the metal ion guests (via the S atom or the π bonds). The richly reactive propynyl units (with potential tautomerization into the propadiene form) can also polymerize to form conjugated polymer components to stabilize and electronically crosslink the MOF host.

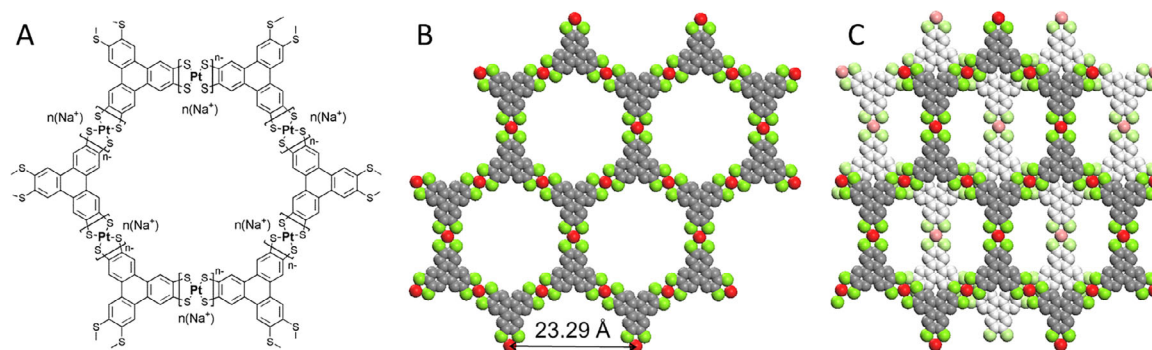


Figure 7. A) Schematic drawing of the honeycomb net of HTT-Pt. B) A single net from a crystal structure model based on standard bonding geometries. C) Two neighboring sheets showing their staggered alignment. The Na⁺ ions are not included in the model.

The Intriguing Field of Coordination Heteroepitaxy: The precise LbL deposition of the LPE protocol offers flexible sequence control to achieve oriented layers with well-defined vertical compositional gradients. As illustrated in the above example of Figure 3, sequential SURMOF deposition allows the cross-linkable (fiber-forming) sheet to be sandwiched by non-crosslinkable (sacrificial) layers, thereby achieving planar 2D fabrics. Furthermore, the alternate growth of one cycle of cross-linkable SURMOF and one cycle of sacrificial SURMOF can also be implemented using the LPE method. While such a prearrangement of active and sacrificial layers is difficult to achieve in conventional solvothermal MOF synthesis, the SURMOF protocol allows this type of multi-heteroepitaxy in a straightforward fashion in which different types of MOFs are stacked to obtain crystalline oriented heterolayers.

Heteroepitaxy is a widely used, industrialized method for processing inorganic electronic materials, e.g., to deposit conductive or semiconductive layers alternating with insulating layers. Here, we illustrate the great potential of the SURMOF approach for achieving advanced heteroepitaxial electronic materials of coordination solids. As electronically conductive coordination networks are relatively rare, we start with an example of processing into SURMOF thin films by the LPE method.

In 2017, Xu and co-workers reported the fabrication of SURMOFs of the type Cu₃(HHTP)₂, (HHTP: 2,3,6,7,10,11-hexahydroxytriphenylene) by employing a spray LPE LbL method, as shown in Figure 6.^[50] The electrically conductive Cu₃(HHTP)₂ SURMOFs exhibited a high degree of orientation, good crystallinity, large single-crystal domain sizes, dense packing, and a smooth surface. Its thickness was tunable by adjusting the number of cycles. The room temperature conductivity of the Cu₃(HHTP)₂ SURMOF with 20 nm thickness was 0.02 S cm⁻¹.

Compared with the catechol oxygen donors of HHTP, sulfur atoms are softer and more polarizable; therefore, the metal-thiolate bonds are of higher covalent character and conducive to stronger electronic interactions in the solid state. Indeed, HHTP's sulfur analogs of 2,3,6,7,10,11-hexathiatriphenylene (HTT, Figure 7) and hexathiobenzene (HTB) have extensively been used to form coordination solids with distinct electronic properties, such as ferromagnetic coupling and band-like/metallic charge transport.^[43–46] Such studies are mostly conducted in the bulk powder form, while SURMOF thin films based on HTT, HTB, or other thiol linkers have not been reported.

The lack of such SURMOF constructs can be ascribed to the air sensitivity of the thiol linkers and the stronger metal-thiol bonding, which makes it more challenging to assemble the metal-sulfur networks in ordered form. For example, one needs to exclude air and carefully choose the solvents and reaction conditions, as illustrated by a recent recipe using *t*-butoxide for in situ deprotection.^[51] But the technology for depositing SURMOF thin films is a fast-moving field. With ever improving protocols for accessing stronger framework systems, it is reasonable to expect high-quality metal-sulfur SURMOF films to be achieved in the near future.

Accelerating the Optimization of Thin-Film Deposition Conditions: When adapting synthesis conditions from bulk MOFs to LbL deposition of MOF thin films, a key issue arises—temperatures for the LbL synthesis are typically significantly lower than those used in the corresponding solvothermal bulk synthesis. Consequently, SURMOF synthesis is governed by kinetic control, making it challenging to determine optimal conditions for producing highly crystalline and oriented films on functionalized substrates. Furthermore, reductions in film roughness and defect density are critical for device integration and the construction of MOF heterostructures. The optimization process typically involves more than seven parameters, and this number increases when accounting for the different deposition parameters between the initial layers (where quasi-heteroepitaxy occurs on a functionalized substrate) and the subsequent homoepitaxial

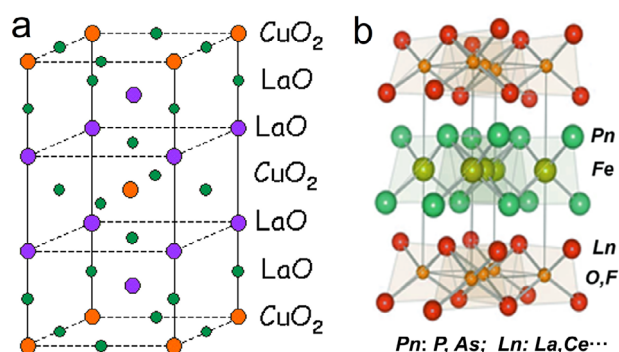


Figure 8. a) Alternating layers in cuprate and iron pnictide superconductors. b) The charge transport layers (transition metal with d electrons) and charge storage layers (no d electrons).

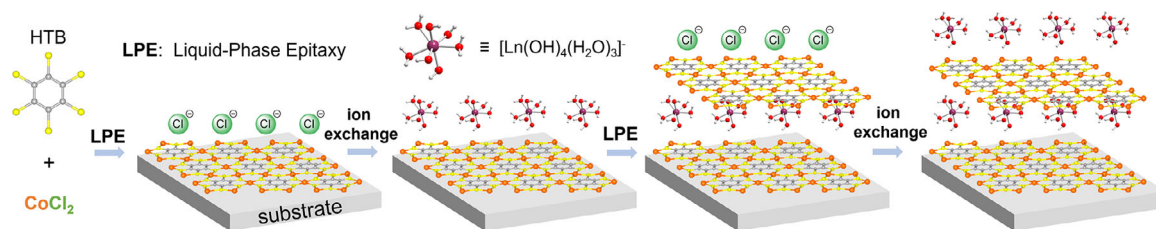


Figure 9. A schematic for an iterative (LbL), liquid-phase epitaxy (LPE) deposition of a SURMOF thin film based on covalent metal-benzenehexathiols (HTB) sheets alternating with ionic lanthanide aqua/hydroxide layers. The initial counterions (e.g., Cl^-) of the thiolate layer (e.g., $\text{Co}_3(\text{C}_6\text{S}_6)^{n+}$) is exchanged with Ln aqua-hydroxide ions to forge the Ln–O layer for potential charge storage function.

growth that enhances SURMOF thickness. Even more parameters will need to be optimized for hetero-epitaxial growth of SURMOFs.

Traditionally, the optimization of synthesis conditions for SURMOF deposition was conducted through trial-and-error methods. These approaches are so time-consuming that a systematic optimization typically was not possible. However, recent advancements have shown that combining machine learning (ML) techniques with robotic synthesis in controlled environments provides a systematic approach to determining the optimal synthesis conditions. This method has been successfully used for a prototype MOF, HKUST-1, effectively directing growth orientation,^[52] minimizing surface roughness,^[53] and optimizing membrane performance.^[54] Looking ahead, we anticipate that these robot-assisted ML methods will continue to evolve and become integral in enhancing the performance of SURMOF-based devices using the new concepts presented in this paper, particularly with optoelectronics and sensor applications.

With such an optimistic perspective, we propose an intriguing layered motif consisting of covalent/conductive layers alternating with ionic/insulating layers. In the traditional inorganic regime, this motif underlies the working mechanism of the high-temperature superconductors of cuprates^[55] and iron pnictides^[56] (Figure 8). It has also been widely studied by the elaborate vapor-phase epitaxy growth apparatus.^[57] In the field of coordination solids, electrically conductive sheets can be formed from the above-mentioned metal–catechol and thiolate systems, but remain overall a rare occurrence—and it is even rarer for the conductive coordination sheets to intercalate with ionic/insulating (e.g., metal oxide) layers.^[58] The lack of such alternating layers in coordination solids calls for closer attention and serious effort from the busy heterogeneous community of framework materials. However, the adaptable paradigm of LPE yielding SURMOFs is particularly effective for creating such intricate layered structures (Figure 9). Undoubtedly, managing the numerous synthesis parameters essential for depositing these multilayers while maintaining the quality of the heterointerfaces will pose challenges. Nevertheless, we anticipate that employing the discussed ML-based robotic synthesis techniques will enable us to surmount these difficulties.

One strong tendency for the planar dithiolene linkers such as HTT and HTB is to form layered coordination structures, e.g., the honeycomb net (Figure 7). Depending on the ligand/metal ratio and the degree of oxidation, the coordination sheets (e.g., with Pt^{2+} , Ni^{2+} , Co^{2+} , and Fe^{2+} metal ions) can bear negative or positive charges, which are, in the initial as-

made form, balanced by the simple cations (e.g., Na^+) or anions (e.g., Cl^-). Of interest would be to replace these simple counterions with more sophisticated metal-aqua/hydroxide ionic components, e.g., $\text{Ln}(\text{OH})_2(\text{H}_2\text{O})_5^+$ or $\text{Ln}(\text{OH})_4(\text{H}_2\text{O})_3^-$. Here, one may prefer metal ions without electronically and magnetically active *d* electrons (e.g., Ln^{3+} , Sc^{3+} , Sr^{2+}), so they can serve distinctly as charge storage domains. The resulting alternating conductive metal–thiolate and metal-aqua/hydroxide layers would then constitute a coordination counterpart of the layered motifs in the superconductors of cuprate and iron pnictides. Even though one can also try directly accessing the alternate thiolate/oxo layers in the bulk phase, the sequential LbL protocol of LPE enabled by the SURMOF paradigm offers advantages. For example, one can first deposit a single layer of HTB-Co $\text{Co}_3(\text{C}_6\text{S}_6)\text{Cl}_n$ onto the SURMOF substrate, and then use ion exchange with the Ln^{3+} species—at an optimized pH—to deposit the $\text{Ln}(\text{OH})_4(\text{H}_2\text{O})_3^-$ components (Figure 9). The cycle can be reiterated to target specific film thicknesses. Similar protocols, with careful adjustments, can be applied for accessing and modifying the heteroepitaxy films of other alternating layer motifs (including recent examples suggesting superconductive potentials^[58]), or for achieving superhydrophobic surfaces with tunable water adhesion strength.^[59]

Note

While this paper was in press, a breakthrough in SURMOF research was reported, wherein high-quality thin films featuring Dirac-cone induced metallic conductivity was achieved through robotic, AI-based layer-by-layer assembly in a self-driving laboratory (DOI: <https://doi.org/10.1039/d5mh00813a>; Mater. Horiz., 2025, 12, 6189). This report highlights an effective combination of theoretical modeling and automated synthesis as enabled by the SURMOF platform, opening up new perspectives for the use of MOFs in future electronics.

Acknowledgements

Z.X. acknowledges an International Excellence Fellowship from Karlsruhe Institute of Technology. C.W. and S.B. acknowledge funding from the SPP Coornet funded by the DFG. The authors thank Mr. Hua-Qun Zhou for helping prepare Figure 9.

Open access funding enabled and organized by Projekt DEAL.

Conflict of Interest

The authors declare no conflict of interest.

Keywords

conductive coordination solids, layer-by-layer (LbL) assembly, Machine Learning, organic quantum materials, surface-mounted metal-organic frameworks (SURMOF)

Received: December 18, 2024

Revised: March 27, 2025

Published online:

- [1] D. J. E. Murdock, *Biol. Rev.* **2020**, *95*, 1372.
- [2] P. U. P. A. Gilbert, K. D. Bergmann, N. Boekelheide, S. Tambutté, T. Mass, F. Marin, J. F. Adkins, J. Erez, B. Gilbert, V. Knutson, M. Cantine, J. O. Hernández, A. H. Knoll, *Sci. Adv.* **2022**, *8*, eab9653.
- [3] J. H. Liu, C. Huang, H. Wu, Y. Long, X. Tang, H. Li, J. Shen, B. Zhou, Y. Zhang, Z. Xu, J. Fan, X. C. Zeng, J. Lu, Y. Y. Li, *Sci. Adv.* **2024**, *10*, adk5047.
- [4] X. Tang, Y. T. Cheng, J. Shen, J. H. Liu, Z. Zhang, Z. Deng, F. Lyu, Y. Yang, G. Zhu, Z. Xu, J. Lu, Y. Y. Li, *Adv. Eng. Mater.* **2023**, *25*, 2300430.
- [5] V. L. H. Tassev, *Crystals* **2017**, *7*, 178.
- [6] H. Gu, J. Xia, C. Liang, Y. Chen, W. Huang, G. Xing, *Nat. Rev. Mater.* **2023**, *8*, 533.
- [7] D. B. Mitzi, *Prog. Inorg. Chem.* **1999**, *48*, 1.
- [8] C. R. Kagan, D. B. Mitzi, C. D. Dimitrakopoulos, *Science* **1999**, *286*, 945.
- [9] J. He, S. Cheng, Z. Xu, *Chem. – A Eur. J.* **2019**, *25*, 8654.
- [10] C. Robl, A. Weiss, *Mater. Res. Bull.* **1987**, *22*, 373.
- [11] B. F. Hoskins, R. Robson, *J. Am. Chem. Soc.* **1989**, *111*, 5962.
- [12] M. Kondo, T. Yoshitomi, K. Seki, H. Matsuzaka, S. Kitagawa, *Angew. Chem., Int. Ed. Engl.* **1997**, *36*, 1725.
- [13] S. S. Y. Chui, S. M. F. Lo, J. P. H. Charmant, A. G. Orpen, I. D. Williams, *Science* **1999**, *283*, 1148.
- [14] H. Li, M. Eddaoudi, M. O'Keeffe, O. M. Yaghi, *Nature* **1999**, *402*, 276.
- [15] X. C. Huang, J. P. Zhang, X. M. Chen, *Chin. Sci. Bull.* **2003**, *48*, 1531.
- [16] J. H. Cavka, S. Jakobsen, U. Olsbye, N. Guillou, C. Lamberti, S. Bordiga, K. P. Lillerud, *J. Am. Chem. Soc.* **2008**, *130*, 13850.
- [17] K. L. Kollmannsberger, L. Kronthaler, J. R. Jinschek, R. A. Fischer, *Chem. Soc. Rev.* **2022**, *51*, 9933.
- [18] M. D. Allendorf, R. Dong, X. Feng, S. Kaskel, D. Matoga, V. Stavila, *Chem. Rev.* **2020**, *120*, 8581.
- [19] C. Wang, D. Liu, W. Lin, *J. Am. Chem. Soc.* **2013**, *135*, 13222.
- [20] T. Drake, P. F. Ji, W. B. Lin, *Accounts Chem. Res.* **2018**, *51*, 2129.
- [21] B. Gui, K. Yee, Y. L. Wong, S. M. Yiu, M. Zeller, C. Wang, Z. Xu, *Chem. Commun.* **2015**, *51*, 6917.
- [22] H. Q. Zhou, Y. He, J. Y. Hu, L. H. Chung, Q. Gu, W. M. Liao, M. Zeller, Z. Xu, J. He, *Chem. Commun.* **2021**, *57*, 187.
- [23] S. Wu, Z. Li, M. Li, Y. Diao, F. Lin, T. Liu, J. Zhang, P. Tieu, W. Gao, F. Qi, X. Pan, Z. Xu, Z. Zhu, A. K. Jen, *Nat. Nanotechnol.* **2020**, *15*, 934.
- [24] O. Shekhah, H. Wang, S. Kowarik, F. Schreiber, M. Paulus, M. Tolan, C. Sternemann, F. Evers, D. Zacher, R. A. Fischer, C. Wöll, *J. Am. Chem. Soc.* **2007**, *129*, 15118.
- [25] O. Shekhah, *Materials* **2010**, *3*, 1302.
- [26] D. H. Chen, H. Gliemann, C. Wöll, *Chem. Phys. Rev.* **2023**, *4*, 35.
- [27] T. Hashem, E. P. Valadez Sánchez, P. G. Weidler, H. Gliemann, M. H. Alkordi, C. Wöll, *ChemistryOpen* **2020**, *9*, 524.
- [28] H. F. Zhang, M. Zhao, Y. S. Lin, *Microporous Mesoporous Mat* **2019**, *279*, 201.
- [29] L. Heinke, Z. G. Gu, C. Wöll, *Nat. Commun.* **2014**, *5*, 6.
- [30] A. A. Talin, A. Centrone, A. C. Ford, M. E. Foster, V. Stavila, P. Haney, R. A. Kinney, V. Szalai, F. El Gabaly, H. P. Yoon, F. Léonard, M. D. Allendorf, *Science* **2014**, *343*, 66.
- [31] Q. Luo, Y. H. Zhong, L. H. Chung, Z. Jiang, Q. C. Lin, X. Xu, X. Ye, W. M. Liao, J. He, *J. Mater. Chem. A* **2023**, *11*, 22223.
- [32] Y. L. Hou, M. Li, S. Cheng, Y. Diao, F. Vilela, Y. He, J. He, Z. Xu, *Chem. Commun.* **2018**, *54*, 9470.
- [33] Z. Xu, *Chem. Lett.* **2021**, *50*, 627.
- [34] X. Ye, L. H. Chung, K. Li, S. Zheng, Y. L. Wong, Z. Feng, Y. He, D. Chu, Z. Xu, L. Yu, J. He, *Nat. Commun.* **2022**, *13*, 6116.
- [35] Z. Wang, A. Blaszczyk, O. Fuhr, S. Heissler, C. Wöll, M. Mayor, *Nat. Commun.* **2017**, *8*, 14442.
- [36] Z. Xu, S. Lee, Y.-H. Kiang, A. B. Mallik, N. Tsomaia, K. T. Mueller, *Adv. Mater.* **2001**, *13*, 637.
- [37] M. Tsotsalas, J. Liu, B. Tettmann, S. Grosjean, A. Shahnas, Z. Wang, C. Azucena, M. Addicoat, T. Heine, J. Lahann, J. Overhage, S. Bräse, H. Gliemann, C. Wöll, *J. Am. Chem. Soc.* **2014**, *136*, 8.
- [38] Z. Hassan, E. Spuling, D. M. Knoll, S. Bräse, *Angew. Chem.-Int. Edit.* **2020**, *59*, 2156.
- [39] R. Patra, S. Mondal, D. Sarma, *Dalton Trans.* **2023**, *52*, 17623.
- [40] H. J. Reich, D. J. Cram, *J. Am. Chem. Soc.* **1967**, *89*, 3078.
- [41] Z. Hassan, E. Spuling, D. M. Knoll, J. Lahann, S. Bräse, *Chem. Soc. Rev.* **2018**, *47*, 6947.
- [42] D. Varadharajan, K. Nayani, C. Zippel, E. Spuling, K. C. Cheng, S. Sarangarajan, S. Roh, J. Kim, V. Trouillet, S. Bräse, N. L. Abbott, J. Lahann, *Adv. Mater.* **2022**, *34*, 12.
- [43] J. Cui, Z. Xu, *Chem. Commun.* **2014**, *50*, 3986.
- [44] R. Dong, P. Han, H. Arora, M. Ballabio, M. Karakus, Z. Zhang, C. Shekhar, P. Adler, P. S. Petkov, A. Erbe, S. C. B. Mannsfeld, C. Felser, T. Heine, M. Bonn, X. Feng, E. Cánovas, *Nat. Mater.* **2018**, *17*, 1027.
- [45] R. Dong, Z. Zhang, D. C. Tranca, S. Zhou, M. Wang, P. Adler, Z. Liao, F. Liu, Y. Sun, W. Shi, Z. Zhang, E. Zschech, S. C. B. Mannsfeld, C. Felser, X. Feng, *Nat. Commun.* **2018**, *9*, 2637.
- [46] X. Huang, S. Zhang, L. Liu, L. Yu, G. Chen, W. Xu, D. Zhu, *Angew. Chem., Int. Ed.* **2018**, *57*, 146.
- [47] K. Yee, N. Reimer, J. Liu, S.-Y. Cheng, S.-M. Yiu, J. Weber, N. Stock, Z. Xu, *J. Am. Chem. Soc.* **2013**, *135*, 7795.
- [48] F. Barthels, G. Marincola, T. Marciniak, M. Konhäuser, S. Hammerschmidt, J. Bierlmeier, U. Distler, P. R. Wich, S. Tenzer, D. Schwarzer, W. Ziebuhr, T. Schirmeister, *ChemMedChem* **2020**, *15*, 839.
- [49] D. Gao, H. Zhai, M. Parvez, T. G. Back, *J. Org. Chem.* **2008**, *73*, 8057.
- [50] M. S. Yao, X. J. Lv, Z. H. Fu, W. H. Li, W. H. Deng, G. D. Wu, G. Xu, *Angew. Chem.-Int. Edit.* **2017**, *56*, 16510.
- [51] B. Wang, J. Li, M. Ye, Y. Zhang, Y. Tang, X. Hu, J. He, C. C. Li, *Adv. Funct. Mater.* **2022**, *32*, 2112072.
- [52] L. Pilz, C. Natzeck, J. Wohlgemuth, N. Scheuermann, P. G. Weidler, I. Wagner, C. Wöll, M. Tsotsalas, *Adv. Mater. Interfaces* **2023**, *10*, 8.
- [53] L. Pilz, M. Koenig, M. Schwotzer, H. Gliemann, C. Wöll, M. Tsotsalas, *Adv. Funct. Mater.* **2024**, *34*, 9.
- [54] L. Pilz, C. Natzeck, J. Wohlgemuth, N. Scheuermann, S. Spiegel, S. Oßwald, A. Knebel, S. Bräse, C. Wöll, M. Tsotsalas, N. Prasetya, *J. Mater. Chem. A* **2023**, *11*, 24724.
- [55] J. G. Bednorz, K. A. Mueller, *Zeitschrift fuer Physik B: Condensed Matter* **1986**, *64*, 189.
- [56] Y. Kamihara, H. Hiramatsu, M. Hirano, R. Kawamura, H. Yanagi, T. Kamiya, H. Hosono, *J. Am. Chem. Soc.* **2006**, *128*, 10012.
- [57] J. Nordlander, M. A. Anderson, C. M. Brooks, M. E. Holtz, J. A. Mundy, *Appl. Phys. Rev.* **2022**, *9*, 17.
- [58] J. He, X. Ye, Z. Liu, L. Tang, J. Hu, Z. Xu, *Mater. Res. Lett.* **2022**, *10*, 496.
- [59] E. Bogdanova, M. Liu, P. Hodapp, A. Borbora, W. Wenzel, S. Bräse, A. Jung, Z. Dong, P. A. Levkin, U. Manna, T. Hashem, C. Wöll, *Mater. Horiz.* **2025**, *12*, 1274.